Isothermal crystallization kinetics and melting behavior of nylon/saponite and nylon/montmorillonite nanocomposites

ARTICLE *in* JOURNAL OF APPLIED POLYMER SCIENCE · DECEMBER 2004

Impact Factor: 1.77 · DOI: 10.1002/app.21167

3 AUTHORS, INCLUDING:

Tzong-Ming Wu
National Chung Hsing University
123 PUBLICATIONS **2,514** CITATIONS

SEE PROFILE

yi-hsin Lien
National Health Research Institutes
4 PUBLICATIONS **108** CITATIONS

SEE PROFILE

Isothermal Crystallization Kinetics and Melting Behavior of Nylon/Saponite and Nylon/Montmorillonite Nanocomposites

Tzong-Ming Wu, Yi-Hsin Lien, Sung-Fu Hsu

Department of Material Science and Engineering, National Chung Hsing University, Taiwan

Received 4 November 2003; accepted 9 June 2004
DOI 10.1002/app.21167
Published online in Wiley InterScience (www.interscience.wiley.com).

ABSTRACT: DSC thermal analysis and X-ray diffraction have been used to investigate the isothermal crystallization behavior and crystalline structure of nylon 6/clay nanocomposites. Nylon 6/clay has prepared by the intercalation of ε-caprolactam and then exfoliating the layered silicates by subsequent polymerization. The DSC isothermal results reveal that introducing saponite into the nylon structure causes strongly heterogeneous nucleation induced change of the crystal growth process from a two-dimensional crystal growth to a three dimensional spherulitic growth. But the crystal growth mechanism of nylon/montmorillonite nanocomposites is a mixed two-dimensional and three-dimensional spherulitic growth. The activation energy drastically decreases with the presence of 2.5 wt % clay in nylon/clay nanocomposites and then slightly increases with increasing clay content. The result indicates that the addition of clay into nylon induces the heterogeneous nucleation (a lower ΔE) at lower clay content and then reduces the transportation ability of polymer chains during crystallization processes at higher clay content (a higher ΔE). The correlation among crystallization kinetics, melting behavior, and crystalline structure of nylon/clay nanocomposites is also discussed. © 2004 Wiley Periodicals, Inc. J Appl Polym Sci 94: 2196–2204, 2004

Key words: nylon 6; nanocomposite; saponite; montmorillonite; Avrami exponent

INTRODUCTION

Nylon 6 is a highly crystalline polymer with two crystalline forms, α and γ.[1–4] The monoclinic α phase is composed of fully extended planar zigzag chain conformation, in which adjacent antiparallel chains are joined to each other by the hydrogen bond. Therefore, it is the thermodynamically most stable crystalline form, and can be obtained by slowly cooling from the melt. The pseudohexagonal γ phase consists of pleated sheets of parallel chains joined by the hydrogen bond. It is less stable and can be obtained by fast cooling from the melt or fiber spinning at a high speed.[5,6] The γ form can be converted into α by recrystallization, by applying stress at room temperature, and by thermal annealing in a saturated-steam atmosphere without any significant loss of orientation.[7–12]

Polymer nanocomposites defined by the particle size of the dispersed phase containing at least one dimension in the range of $1 \sim 100$ nm have received increasing interest due to their unusual combinations of stiffness and toughness that are difficult to attain from individual components.[13–15] Typical preparation of polymer nanocomposites is either intercalation of a suitable monomer and then exfoliating the layered silicate host into their nanoscale elements by subsequent polymerization, or direct insertion of polymer chains from the melt or solution into swellable layer silicate.[16–18] The high aspect ratio layered silicate would affect the physical, mechanical, and thermal properties of the synthesizing polymer nanocomposites.

In this study, we have used two different types of clays, montmorillonite and saponite, as the dispersed phase to prepare nylon 6/clay nanocomposites. The montmorillonite is dioctahedral smectites with predominantly octahedral substitution, while saponite is trioctahedral smectites with mainly the isomorphous substitution of Si^{4+} by Al^{3+} in the tetrahedral sheets. For this reason, the structure of montmorillonite is in the form of hexagonal lamellae, while the saponite shows a structure in the form of ribbons and laths.[19] The nylon 6/clay nanocomposites were prepared through the intercalation of ε-caprolactam and then exfoliating the layered clay by subsequent polymerization.[20,21] Both X-ray diffraction data and transmission electron microscopy micrograph of nylon/clay nanocomposites indicate most of the swellable silicate layers are exfoliated into the nylon matrix. X-ray dif-

Correspondence to: T.-M. Wu (tmwu@dragon.nchu.edu.tw).
Contract grant sponsor: NSC; contract grant number: NSC92–2622-E-005–006-CC3.

fraction data also show the presence of polymorphism in nylon/clay nanocomposites, which is strongly dependent on the annealing temperature of nylon/clay nanocomposites and on the content of clay in nylon/clay nanocomposites. The mechanical and thermal properties of nylon 6/clay nanocomposites are also significantly affected by the addition of clay,[20–23] which is probably due to the different structural features of saponite and montmorillonite. Therefore, different types of clays containing their special structure arrangement probably play a significant role to affect their physical and thermal properties. Since the physical properties of nanocomposites are also directly related to the crystalline features and thermal behaviors, it is necessary to understand the effect of clays on the crystallization behaviors of nylon 6/clay nanocomposites.

In this study, we have focused on the isothermal melt-crystallization kinetics, melting behavior, and crystalline structure of nylon 6 with the presence of saponite and montmorillonite from DSC and X-ray diffraction method. The parameters of crystallization kinetics, such as the laternal-surface and fold-surface energy of isothermal crystallization as well as the activation energy of isothermal crystallization of nylon and nylon/clay nanocomposites is also discussed.

EXPERIMENTAL

Specimens

Saponite (SA) and montmorillonite (MMT) with a cation exchange capacity (CEC) of 80 and 110 meq/100 g, respectively, were used as the dispersed phase to reinforce the nylon matrix. The nylon 6/clay nanocomposite has been prepared by using ε-caprolactam mixed with deionized water, phosphoric acid solution, and organically modified clay using octadecylammonium at 80°C for 30 min. The polymerization was carried out in a nitrogen atmosphere by heating the mixture to 270°C, while stirring for 30 min with the pressure being elevated to 8 kg/cm^2. The pressure was then reduced to 1 kg/cm^2, and the mixture was polymerized at 260°C for 6 h. Upon the completion of the polymerization, the reinforced nylon 6/clay nanocomposite was taken out from the reactor and cut into pellets. The pellets thus obtained were washed with hot water at 80°C for 8 h and dried at 100°C for 12 h in vacuum.

Samples of pure nylon and nylon/clay nanocomposites were sandwiched between two cover glasses and heated on a hot stage at premelting temperature (T_{max}) of 240°C. The sample was pressed into the thin film with thickness in the range of 0.03 mm, kept for 20 min to eliminate any thermal history and the memory of crystalline form in the melt, and then quenched rapidly to their room temperature at a cooling rate (C) in the range of 1 ~ 50°C/min.

Wide angle X-ray diffraction

X-ray $\theta/2\theta$ diffraction scans of these specimens were obtained using a 3kW Rigaku III diffractometer equipped with Ni-filtered CuKα radiation. These data were recorded in the reflection mode.

Thermal analysis

Thermal analysis of the samples was preformed using a Perkin–Elmer PYRIS Diamond differential scanning calorimeter (DSC) calibrated using indium, and all experiments were carried out under a nitrogen atmosphere. All specimens were weighted in the range of 5 to 6 mg. For isothermal crystallization, the specimens were heated to T_{max} = 240°C at a rate of 100°C/min and held for 20 min to remove the residual crystals, then they were quickly cooled to the proposed crystallization temperatures (T_{cs}) in the range of 199 ~ 207°C. Heat fusion versus time for isothermal crystallization (ΔH_c) was recorded. Therefore, the glass transition temperature (T_g), crystallization temperature (T_c), exothermic heat of crystallization (ΔH_c), crystalline melting temperature (T_m), and heat of fusion of polymer crystalline (ΔH_m) for the nylon and nylon/clay nanocomposites were obtained. The specimens isothermally crystallized at the T_{cs} were heated to T_{max} = 240°C at a rate of 10°C/min.

Thermal treatment

For the thermal treatment experiment, samples of pure nylon and nylon 6/clay nanocomposites were hot pressed into thin film at 240°C and then were transferred quickly from the hot stage to a silicon oil bath kept at the range between 199 and 207°C for various times.

RESULTS AND DISCUSSION

The crystallization kinetics of nylon and nylon/clay nanocomposites can be analyzed by using the classical Avrami equation[24,25] as given in eq. (1).

$$1 - X_t = \exp(-kt^n) \tag{1}$$

where X_t is the development of crystallinity X_c at time t. The fraction of X_t is obtained from the area of the exothermic peak in DSC isothermal crystallization analysis at a crystallization time t divided by the total area under the exothermic peak.

$$X_t = \frac{\int_0^t \frac{dH}{dt} dt}{\int_0^\infty \frac{dH}{dt} dt} = \frac{\Delta H_t}{\Delta H_0} \tag{2}$$

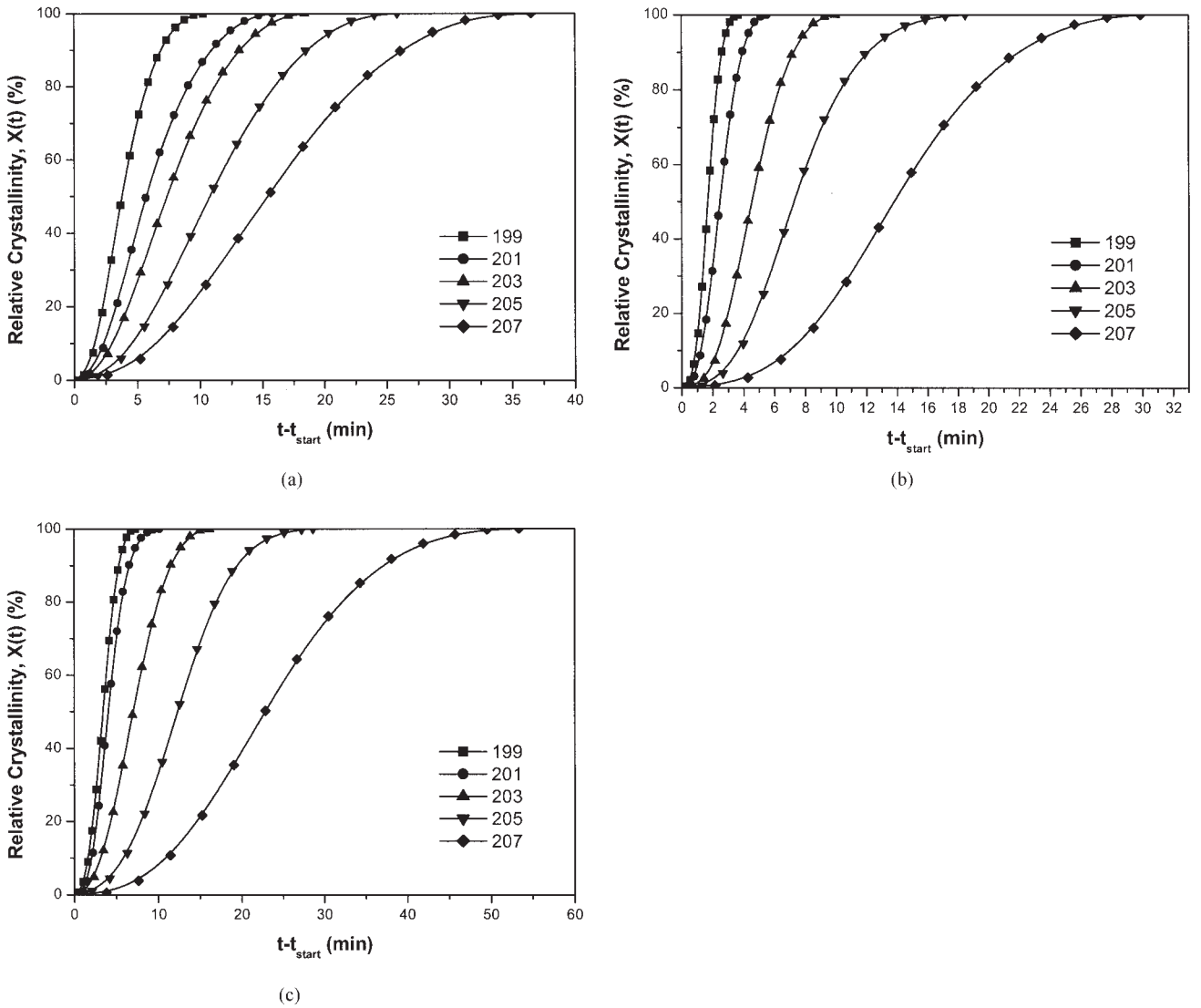

Figure 1 Development of crystallinity with time for (a) nylon, (b) 2.5 wt % nylon/SA, and (c) 5 wt % nylon/SA nanocomposites during isothermal crystallization.

where the numerator is the heat (ΔH_t) generated at time t and the denominator is the total heat (ΔH_0) generated up to the complete crystallization. Figure 1 shows the development of crystallinity with time in nylon and 2.5 wt % and 5 wt % nylon/SA nanocomposites at five different crystallization temperatures. All these curves show similar sigmoid shape, which indicates crystallization procedure was similar at each crystallization temperature. In eq. (1), the k value is the crystallization rate constant (min^{-1}) and n value is the Avrami exponent. Both k and n depend on the nucleation and growth mechanisms of spherulites. To convert conveniently with the operation, eq. (1) can be transformed into

$$\ln[-\ln(1 - X_t)] = n \ln t + \ln k \quad (3)$$

Figure 2 shows the plot of ln [-ln (1-X_t)] versus ln t for nylon and 2.5 wt % and 5 wt % nylon/SA nanocomposites. The k and n values could be directly obtained using eq. (3) from the intercept and slope of the best-fitting line. It is usual to distinguish the crystallization behavior at the linear stage, that is, before the kinetic curve deviates markedly from the theoretical isotherms and the primary crystallization and the secondary crystallization occur at the nonlinear stage. The primary crystallization consists of the outward growth of lamellar stacks until impingement; and the secondary crystallization, which may well overlap the primary crystallization, is filling in the spherulites of interstices. Many results have been suggested that both primary and secondary crystallization were incorporated into Avrami theory. In the present work, we focus only on primary crystallization. Several crystallization parameters, ΔH_0, k and n, are summarized in Table I. The plots of ln [-ln (1-X_t)] versus ln t for 2.5 wt % nylon/MMT and 5 wt % nylon/MMT show similar tendency, and their crystallization parameters

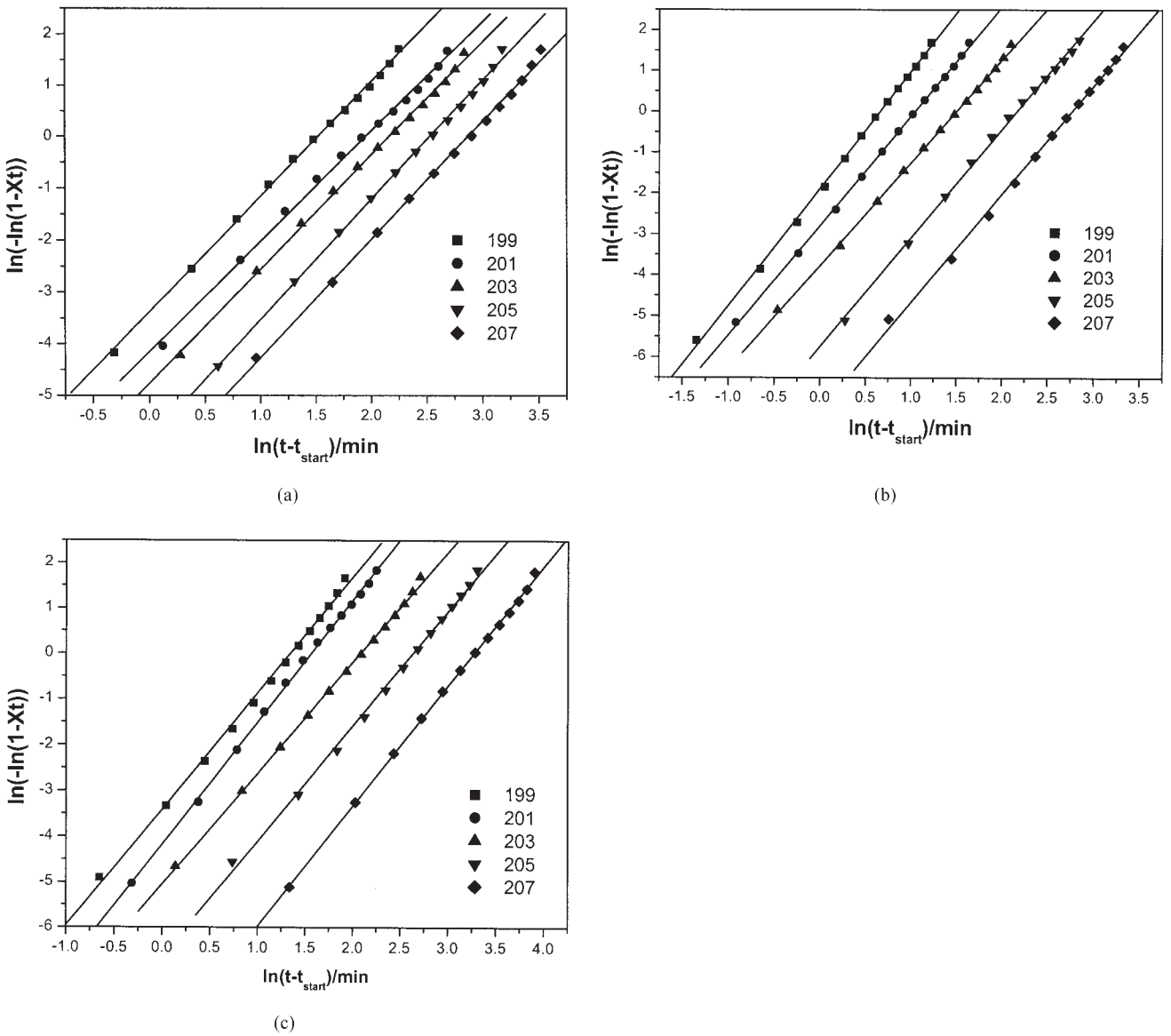

Figure 2 Avrami plots of ln [-ln (1-X_t)] versus ln t for (a) nylon, (b) 2.5 wt % nylon/SA, and (c) 5 wt % nylon/SA nanocomposites.

are also listed in Table I. It is found n values are dependent on the content of clay and T_c.

For the nylon sample, the n values range around 2.1 ~ 2.3 with increasing T_c. In general, a value of n close to 3 may represent an athermal nucleation process followed by a three-dimensional crystal growth. On the other hand, the value of $n \approx 2.0 \sim 2.2$ indicates that crystal growth may not occur in three dimensions at an equal rate, and hence a low n value may be obtained. The nonintegral n values we obtained might be due to the presence of crystalline branching and/or two stage crystal growth during the crystallization process and/or mixed growth and nucleation mechanism.[26] The n values of 2.5 wt % and 5 wt % nylon/SA nanocomposites are also in the range of 2.5 ~ 2.8, which are higher than those of nylon. These results indicate that introducing 2.5 wt % and 5 wt % of saponite into the nylon structure causes strongly heterogeneous nucleation induced change of the crystal growth process from a two-dimensional crystal growth to a three dimensional spherulitic growth. The n values of 2.5 wt % and 5 wt % nylon/MMT nanocomposites are in the range of 2.3 ~ 2.8, which are also higher than those of nylon. These results indicate that introducing 2.5 wt % and 5 wt % of MMT into the nylon structure causes heterogeneous nucleation induced change of the crystal growth process from a two-dimensional crystal growth to a mixed three-dimensional and two-dimensional spherulitic growth.

In addition, the values of the crystallization rate parameters k are apt to decrease with increasing T_c due to a gradual decrease in the degree of supercool-

TABLE I
Values of t_{start}, k, and n at Various T_c for Nylon 6, Nylon 6/MMT, and Nylon 6/SA Nanocomposites

T_c (°C)	199	201	203	205	207
Nylon 6					
t_{start} (min)	8.44	9.47	10.91	13.69	19.70
ΔH_0 (J/g)	−40.97	−35.73	−28.92	−27.07	−24.19
n	2.23	2.13	2.20	2.32	2.28
k	3.36E-02	1.56E-02	8.46E-03	2.87E-03	1.42E-03
2.5 wt% nylon 6/MMT					
t_{start} (min)	9.44	10.46	13.88	18.52	24.74
ΔH_0 (J/g)	−41.30	−39.56	−36.39	−28.58	−38.66
n	2.66	2.73	2.54	2.48	2.80
k	4.08E-02	1.27E-02	7.86E-03	2.52E-03	8.80E-05
5 wt% nylon 6/MMT					
t_{start} (min)	9.53	10.99	18.44	27.00	43.18
ΔH_0 (J/g)	−41.23	−50.11	−26.47	−25.70	−30.95
n	2.61	2.54	2.43	2.31	2.29
k	6.47E-03	2.76E-03	1.17E-03	7.84E-04	1.61E-04
2.5 wt% nylon 6/SA					
t_{start} (min)	8.21	9.13	11.07	13.15	18.28
ΔH_0 (J/g)	−41.53	−39.55	−34.47	−39.04	−46.29
n	2.87	2.68	2.52	2.66	2.65
k	1.51E-01	6.09E-02	2.29E-02	3.18E-03	6.64E-04
5 wt% nylon 6/SA					
t_{start} (min)	8.86	9.24	12.68	17.00	21.79
ΔH_0 (J/g)	−39.24	−51.12	−36.23	−35.80	−53.02
n	2.55	2.67	2.43	2.52	2.63
k	3.28E-02	1.52E-02	6.35E-03	1.32E-03	1.83E-04

ing, and to increase with increasing clay content due to an increase in the heterogeneous nucleation. The crystallization rates of the 2.5 wt % nylon/SA nanocomposites rapidly decrease as T_c increases, while those of the nylon and the other nylon/clay nanocomposites decrease gradually as T_c increases. At lower crystallization temperatures ($199 \leq T_{cs} \leq 203$°C), the crystallization rate of nylon/clay nanocomposites is higher than that of pure nylon, except for the 5 wt % nylon/MMT nanocomposites. These results indicate that the additional content of clay does affect the crystallization behaviors of the nylon.

The crystallization rate parameter k can also be approximately described as follows:

$$1/n(\ln k) = \ln k_0 - \Delta E_a/\mathrm{RT} \quad (4)$$

where k_0 is a temperature-independent preexponential factor; ΔE_a is a total activation energy, which consists of the transport activation energy ΔE^* and the nucleation activation energy ΔF (ΔE^* refers to the activation energy required to transport molecular segments across the phase boundary to the crystallization surface, and ΔF is the free energy of formation of the critical size crystal nuclei at T_c); and R is the universal gas constant. Arrhenius plots of 1/n (ln k) against 1/T for nylon and nylon/clay nanocomposites are shown in Figure 3, and are approximately linear. The activation energy can be determined from the slope of the plots and is strongly dependent on the content of clay. The activation energy drastically decreases with the presence of 2.5 wt % clay in nylon/clay nanocomposites. The result indicates that the addition of 2.5 wt % SA and MMT into nylon probably induces heterogeneous nucleation (a lower ΔE_a). The addition of more clay into the nylon matrix causes more heterogeneous nucleation, which is expected to obtain a lower ΔE_a. But the addition of more clay also induces more steric hindrance, which also reduces the transportation ability of polymer chains during crystallization processes (a higher ΔE_a), and the ΔE_a of nylon/clay nanocomposites increases as clay content increases from 2.5 wt % to 5 wt %. Detail activation energy of nylon and nylon/clay nanocomposites are shown in Table II.

Figure 4 shows the DSC heating scans of nylon and 2.5 and 5 wt % nylon/SA nanocomposites after completion of isothermal crystallization at various T_c, which are then heated directly from T_c to T_{max} = 240°C at a heating rate of 10°C/min. It can be clearly seen that the DSC heating curves of these specimens contain only two endotherm behaviors. The peak temperature of the first and smallest endotherm (referred to as T_m(I)) is about 5 ~ 10°C above T_c in all figures. The peak position of T_m(I) associated with the last step of secondary crystallization shifts to higher temperature as T_c is increased. The second melting endotherm (referred to as T_m(II)), associated with the fusion of crystals grown at T_c, corresponds to the thermodynamically most stable α crystalline form.

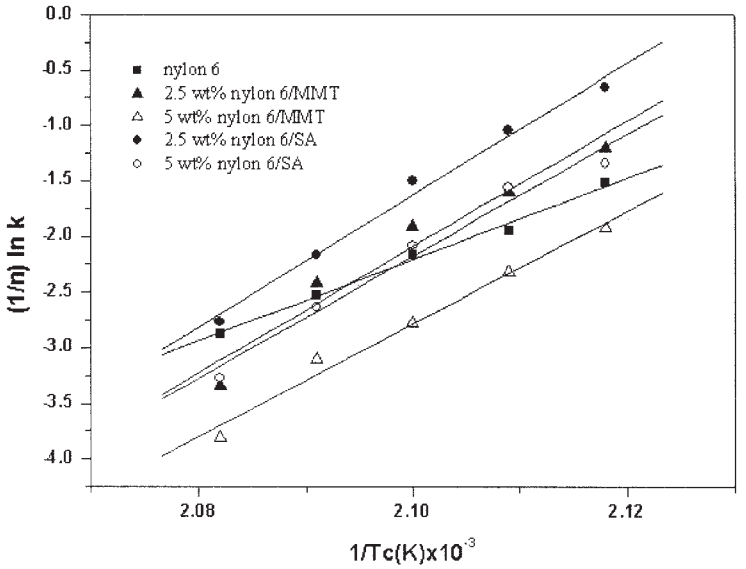

Figure 3 Arrhenius plots of 1/n (ln *k*) versus 1/T for nylon and nylon/clay nanocomposites.

The equilibrium melting temperature T_m^o of the nylon and nylon/clay nanocomposites can be determined by the plot of T_m(II) versus T_c according to Hoffman and Week's equation:[27]

$$T_m = T_m^0(1 - 1/\gamma) + T_c/\gamma \quad (5)$$

where γ is a factor depending on the final laminar thickness. It is assumed that $\gamma = l/l^*$, where l and l^* are the thickness of a mature crystallite and of the critical crystalline nucleus. T_m^o can be determined from the crossing point of the $T_m = T_c$ line with the extrapolation of T_m as a function of T_c. This procedure is equivalent to an extrapolation to infinite lamellar thickness, and the extrapolated equilibrium melting point is 231.2°C for the nylon 6, which is in good agreement with those reported previously.[28,29] The T_m^o is in the range of 227 ~ 231°C for the nylon 6/clay nanocomposites and is also listed in Table II. It can be seen that the T_m^o is close to each other, suggesting that the crystalline in nylon/clay nanocomposites is similar to that of pure nylon.

The regime theory of crystal growth is applied to analyze those crystal growth data to obtain thermodynamic parameters related to the crystallization process. It has to be emphasized that overall crystallization rates are not simple to be interpreted as spherulitic radial growth because of the combination of nucleation and growth phenomena. According to the regime theory of crystal growth, the temperature dependence of the linear growth rate (G) is given as follows:

$$G = G_0 \exp\left[\frac{-U^*}{R(T_c - T_\infty)}\right] \exp\left[\frac{-Kg}{fT_c\Delta T}\right] \quad (6)$$

where G_o is a pre-exponential term; U*, the diffusional activation energy for the transport of crystallizable segments at the liquid-solid interface; T∞, the hypothetical temperature below which viscous flow ceases; $f = 2T_c/(T_m^o + T_c)$, a correction factor that accounts for the change of ΔH_f^o (enthalpy of fusion of the perfect crystal) with the temperature. The nucleation constant K_g contains contributions from the surface free energies, and it can be obtained from eq. (6):

$$Kg(I) = \frac{4b\sigma\sigma_e T_m^0}{\beta k \Delta H_f^0} \text{ or } Kg(II) = \frac{2b\sigma\sigma_e T_m^0}{\beta k \Delta H_f^0} \quad (7)$$

TABLE II
Values of Δ E_a, T_m^0, K_g, G_0 and $\sigma\sigma_e$ at Various T_c for Nylon 6, Nylon 6/MMT, and Nylon 6/SA Nanocomposites

	Nylon 6	2.5 wt % nylon 6/MMT	5 wt % nylon 6/MMT	2.5 wt % nylon 6/SA	5 wt % nylon 6/SA
Δ E_a (kJ/mol)	−302.8	−470.3	−420.0	−492.5	−455.2
T_m^0 (°K)	503.4	503.2	500.1	503.9	503.7
K_g (K^2)	7.37E+04	1.07E+05	7.24E+04	1.14E+05	1.03E+05
G_0	3.87E+03	6.11E+04	4.11E+03	1.35E+05	3.47E+04
$\sigma\sigma_e$ (erg^2/cm^4)	125.0	180.8	123.7	192.4	174.0

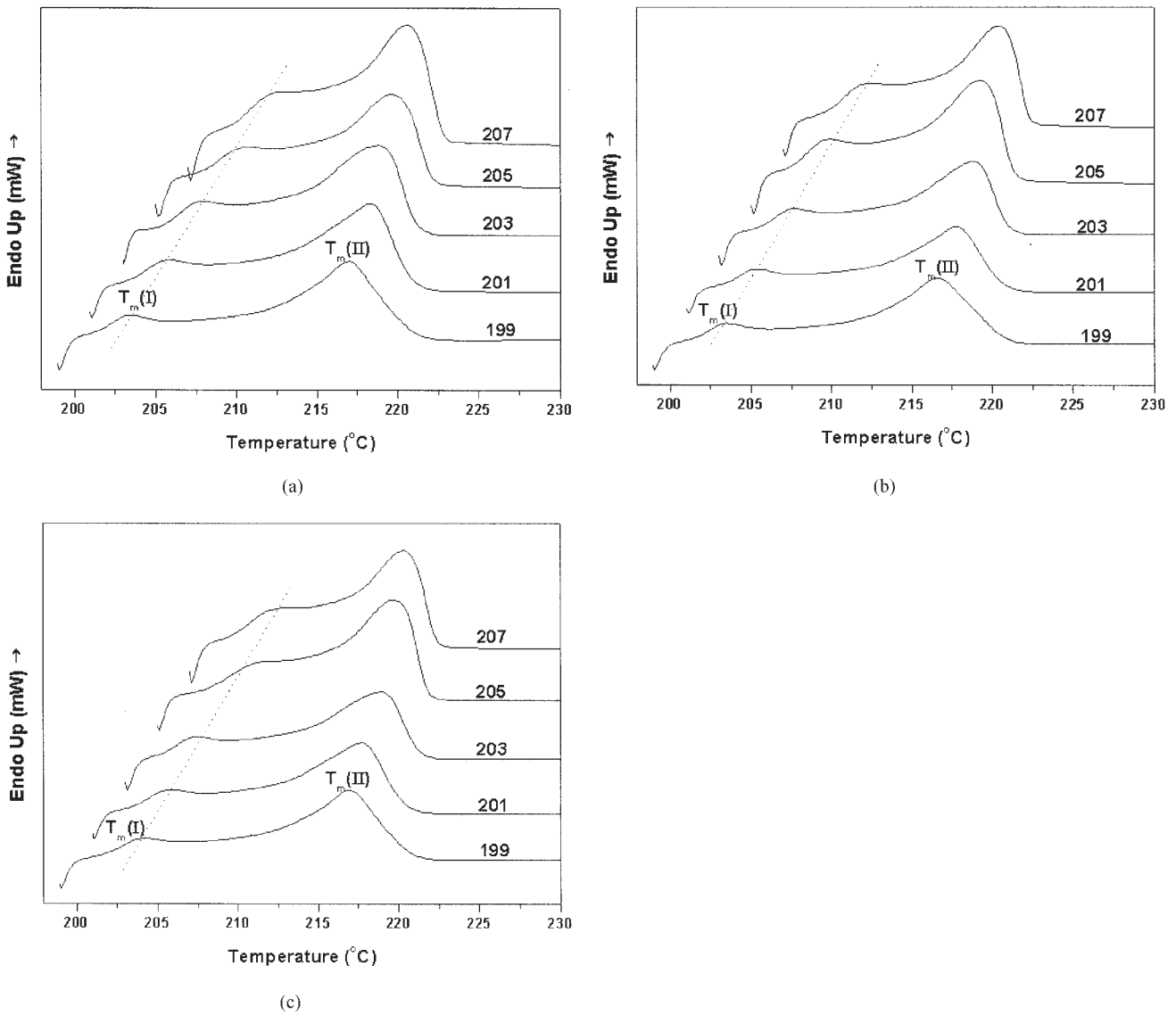

Figure 4 DSC heating curves of (a) nylon, (b) 2.5 wt % nylon/SA, and (c) 5 wt % nylon/SA nanocomposites after completing the isothermal crystallization at various T_c.

where m is a parameter that depends on the regime of crystallization, b is the distance between two adjacent fold planes, σ and σ_e are the lateral and folding surface free energy, and k is the Boltzmann constant. The K_g is equal to K_g(I) when the formation of a surface nucleus is followed by rapid completion of the substrate (regime I kinetics), and K_g is equal to K_g(II) when the surface nuclei form in large numbers on the substrate and spread slowly (regime II kinetics). Using half-time of crystallization $t_{1/2}$ instead of growth rate G, eq. (6) can be rewritten as follows:

$$\ln\left(\frac{1}{t_{1/2}}\right) + \frac{U^*}{R(T_c - T_\infty)} = \ln G_0 - \frac{Kg}{fT_c\,\Delta T} \qquad (8)$$

Hoffman et al.[27,30] found T∞ = Tg - 30 K and U* = 1500 cal mol^{-1} by fitting the crystallization rate data for various polymers with eq. (8).

Figure 5 shows the plots of $\ln(1/t_{1/2}) + U^*/[R\,(T_c - T\infty)]$ versus $1/[f T_c \Delta T]$ for nylon and nylon/clay nanocomposites. The K_g and G_o values obtained from the slope and intercept of Figure 5 are listed in Table II. The data of b of α crystalline form is 1.72 nm according to the lattice parameter of nylon, and the bulky enthalpy of fusion of perfect crystal ΔH_f^o is 190.0 J/g.[31,32] To determine to which regime the data in the selected crystallization temperatures belong, the Lauritzen Z test is usually applied.[33] Z is a quantity defined by

$$Z \approx 10^3 \cdot \left(\frac{L}{2a_0}\right)^2 \exp\left(-\frac{X}{T_c \Delta T}\right) \qquad (9)$$

where L is the effective lamellar width and a_0 is the width of the molecular chain in the crystal. According

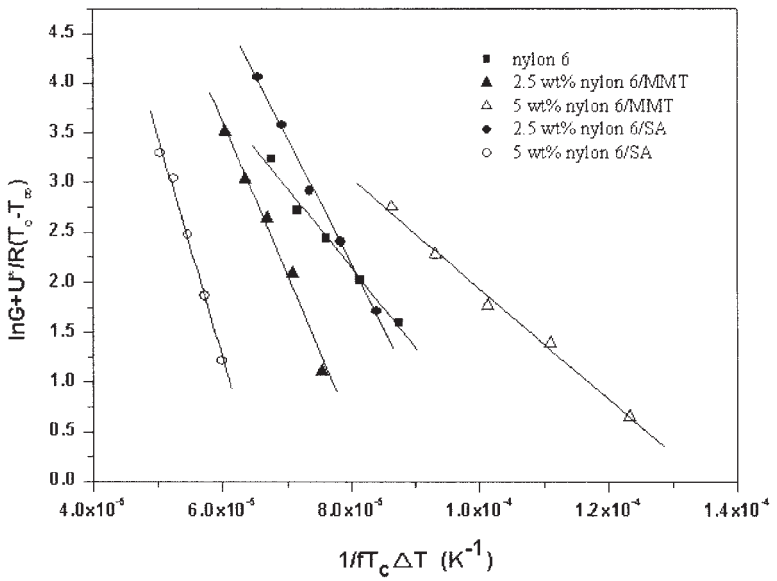

Figure 5 Plots of $\ln(1/t_{1/2}) + U^*/[R(T_c - T\infty)]$ versus $1/[f T\chi\Delta T] \times 10^5$ for nylon and nylon/clay nanocomposites.

to this test, regime I crystallization kinetics are followed if the substitution of $X = K_g$ into the test results in $Z \leq 0.01$. If with $X = 2K_g$ the test contains $Z \geq 1.0$, regime II kinetics are followed. As pointed out by Lauritzen and Hoffman,[34] it is more convenient, given a known value of K_g and the inequalities for Z, to obtain the values of L in regime I or regime II and to estimate if such values of L are realistic. The α crystalline unit cell of nylon 6 is monoclinic with the lattice parameter a = 0.956 nm, b = 0.801 nm, c = 1.72 nm (fiber axis), $\gamma = 67.5°$ containing 4 monomer per unit cell, while the γ crystalline unit cell is pseudohexagonal with the lattice parameter a = 0.472 nm, c = 1.688 nm, $\gamma = 120°$. It will be pointed out later (see Fig. 6) that the crystalline structure in the selected crystallization temperatures is monoclinic. This preferred growth plane will be (200) where the thickness of a monomolecular layer, b_0, in the (100) plane is 0.44 nm and the chain width, a_0, is 0.37nm. Assuming $Z \leq 0.01$ and substituting $X = K_g$ into the Z-test, L will be smaller than 0.03 nm. This is clearly unrealistic. Assuming $Z \geq 1.0$ and substituting $X = 2K_g$ into the Z-test, we obtain $L \geq 3.4$ nm, and it is reasonable for nylon 6. Therefore the crystallization regime is determined to be regime II.

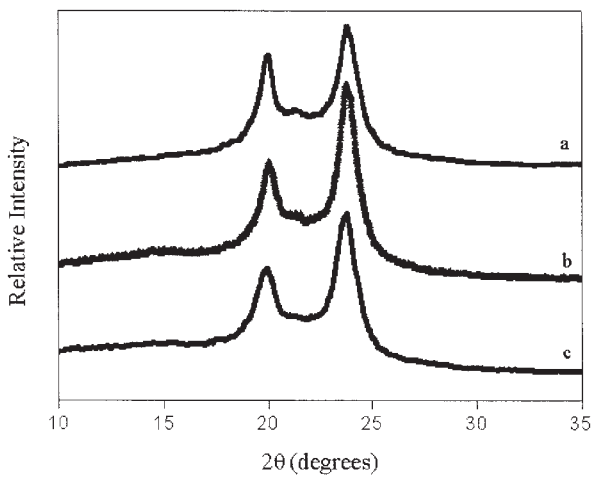

Figure 6 X-ray diffraction data for (a) nylon, (b) 2.5 wt % nylon/SA, and (c) 5 wt % nylon/SA thermally annealed at 205°C.

Because the content of additional clay is low, the parameter of b, ΔH_f^o, and the crystallization regime can be assumed to be the same as those of pure nylon. The $\sigma\sigma_e$ data of the nylon and nylon/clay nanocomposites are also determined from eq. (8) and shown in Table II. These data indicate that 2.5 wt % nylon/SA and nylon/MMT nanocomposites have higher values of G_o, suggesting the introduction of 2.5 wt % SA and MMT into nylon acted as heterogeneous nuclei in the nucleation of crystallization, causing a dramatic increase of the crystallization rate (a higher G_o). The addition of 5 wt % SA and MMT into the nylon matrix could further induce the increase in heterogeneous nucleation, which is expected to obtain a higher G_o. But the addition of SA and MMT into nylon also causes a decrease in free volume and thus a decrease in molecular chain mobility, leading to a lower growth rate constant G_o. Therefore, the addition of 5 wt % SA in the form of ribbons and laths into nylon decreases the molecular chain mobility of nylon, causing a slight increase in growth rate constant G_o compared to that of 2.5 wt % nylon/SA nanocomposites. But the presence of 5 wt % MMT in the form of hexagonal lamellae

dramatically decreases the molecular chain mobility of nylon, causing a sharp decrease in growth rate constant G_o compared to that of 2.5 wt % nylon/MMT nanocomposites. It is clear that the heterogeneous nucleation is a key factor in the crystallization process of 2.5 wt % nylon/clay nanocomposites, but the molecular chain mobility can control the crystallization process for 5 wt % nylon/MMT nanocomposites. The $\sigma\sigma_e$ data of nylon and nylon/clay nanocomposites also show similar trends as those of growth rate constants.

Figure 6 shows X-ray diffraction data of nylon and 2.5 wt % and 5 wt % nylon/clay nanocomposites after melting at 240°C and then quenching to the temperature in the range of 199 ~ 207°C. X-ray data of nylon shows two intense reflections (100) and (010) + (110), at $2\theta \cong 20.5°$ and 24.0° characteristic of the monoclinic α crystalline form. The peak positions of these reflections of nylon/clay nanocomposites are almost equivalent to those of nylon, but the peak profile of nylon/clay nanocomposites are slightly broader than those of the nylon matrix. These results indicate that the nylon and nylon/clay nanocomposites have the same crystalline structure. Therefore, our previous assumption that nylon/clay nanocomposites have the same b of α crystalline form as that of pure nylon matrix is reasonable.

CONCLUSION

DSC isothermal results reveal that introducing saponite into the nylon structure causes strongly heterogeneous nucleation induced change of the crystal growth process from a two-dimensional crystal growth to a three dimensional spherulitic growth. But the crystal growth mechanism of nylon/MMT nanocomposites is a mixed two-dimensional and three-dimensional spherulitic growth. The $\sigma\sigma_e$ data of the nylon and nylon/clay nanocomposites indicate that 2.5 wt % nylon/SA and nylon/MMT nanocomposites have higher values of G_o, suggesting the introduction of SA and MMT into nylon acted as heterogeneous nuclei in the nucleation of crystallization and caused a decrease in free volume at high clay content to reduce the molecular chain mobility.

Financial support provided by NSC through the project NSC92–2622-E-005–006-CC3 was greatly appreciated.

References

1. Miyasaka, K.; Ishikawa, K. J Polym Sci A-2 1968, 6, 1317.
2. Miyasaka, K.; Ishikawa, K. J Polym Sci A-2 1972, 10, 1497.
3. Kyotani, M. J Macromol Sci, Phys 1975, B11, 509.
4. Murthy, N. S. Polym Commum 1991, 32, 301.
5. Brucato, V.; Crippa, G.; Piccarolo, S.; Titomanlio, G. Polym Eng Sci 1991, 31, 1411.
6. Samon, J. M.; Schultz, J. M.; Wu, J.; Hsiao, B.; Yeh, H.; Kolb, R. J Polym Sci, Polym Phys Ed 1999, 37, 1277.
7. Murthy, N. S.; Szollosi, A. B.; Sibilia, J. P.; Krimm, S. J Polym Sci, Polym Phys Ed 1985, 23, 2369.
8. Matyi, R. J.; Cryst Jr., B. J Polym Sci, Polym Phys Ed 1978, 16, 1329.
9. Park, J. B.; Devries, K. L.; Statton, W. O. J Macromol Sci, Phys 1978, B15, 229.
10. Baldrian, J.; Pelzbauer, Z. J Polym Sci Part C 1972, 38, 289.
11. Murthy, N. S.; Minor, H.; Latif, R. A. J Macromol Sci, Phys 1987, B26, 427.
12. Hiramatsu, N.; Hirakawa, S. Polym J 1982, 14, 165.
13. Giannelis, E. P. Adv Mater 1996, 8, 29.
14. Okada, A.; Usuki, A. Mater Sci Eng 1995, C3, 109.
15. Ogawa, M.; Kuroda, K. Bull Chem Soc Jpn 1997, 70, 2593.
16. Lagaly, G. Appl Clay Sci 1999, 15, 1.
17. LeBaron, P. C.; Wang, Z.; Pinnavaia, T. J. Appl Clay Sci 1999, 15, 11.
18. Liu, L.; Qi, Z.; Zhu, X. J Appl Polym Sci 1999, 71, 1133.
19. Usuki, A.; Okada, A. Jap Plastics 1995, 46, 31.
20. Wu, T.-M.; Liao, C. S. Macromol Chem Phys 2000, 201, 2820.
21. Wu, T.-M.; Chen, E.-C.; Liao, C. S. Polym Eng Sci 2002, 42, 1141.
22. Cho, J. W.; Paul, D. R. Polymer 2001, 42, 1083.
23. Fornes, T. D.; Paul, D. R. Polymer 2003, 44, 3945.
24. Avrami, M. J Chem Phys 1939, 7, 1103.
25. Avrami, M. J Chem Phys 1940, 8, 212.
26. Alamo, R. G.; Mandelkern, L. Macromolecules 1991, 24, 6480.
27. Hoffman, J. D.; Weeks, J. J. J Res Nat Bur Stand 1962, 66A, 13.
28. Privalko, V. P.; Kawai, T.; Lipatov, Y. S. Polym J 1979, 11, 699.
29. Ho, J.-C.; Wei, K.-H. Macromolecules 2000, 33, 5181.
30. Hoffman, J. D. Polymer 1983, 24, 3.
31. Cheng, L.-P.; Dwan, A.-H.; Gryte, C. C. J Polym Sci, Polym Phys Ed 1994, 32, 1183.
32. Wunderlich, B. In Macromolecular Physics, Vol. 1; Academic Press: New York, 1973.
33. Lauritzen, J. I. J Appl Phys 1973, 44, 4353.
34. Lauritzen, J. I.; Hoffman, J. D. J Appl Phys 1973, 44, 4340.